OFF-ROAD HANDLING OF A MINI BAJA VEHICLE

Kyle Thomas Winnaar

A dissertation submitted to the Faculty of Engineering and the Built Environment, University of the Witwatersrand, Johannesburg, in fulfilment of the requirements for the degree of Master of Science in Engineering.

Johannesburg 2017

Declaration

I declare that this dissertation is my own, unaided work, except where otherwise acknowledged. It is being submitted for the degree of Master of Science in Engineering in the University of the Witwatersrand, Johannesburg. It has not been submitted before for any degree or examination at any other university.

Signed this 20th day of September 2017

Kyle Thomas Winnaar

Abstract

The primary focus of vehicle dynamics studies have been the handling capabilities and suspension design of a vehicle to achieve the optimal road holding capability and ride comfort level. Numerous studies have focussed on the design, modelling and optimisation for on-road vehicle suspensions, but the study of vehicle dynamics on off-road surfaces is still relatively new. The objectives of this dissertation were to characterise the steady-state cornering response for on-road and off-road surfaces, evaluate the open-loop vehicle response using the step-steering input manoeuvre, and evaluate the closed-loop vehicle response using the double lane change (DLC) manoeuvre of a mini baja vehicle. The mini baja vehicle was instrumented with an inertial measurement unit (IMU) to measure vehicle accelerations and yaw rate, a steering angle sensor, throttle and brake position sensors, and a wheel speed sensor to measure rear wheel angular velocity. A tarmac surface was used as a control test surface, while grass and dirt track surfaces offered decreasing tyre grip levels, resulting in larger sideslip. The handling on the tarmac surface was repeatable for all the cornering tests performed. On the grass and dirt track surface, tyre grip levels decreased, resulting in an increase in steering variability when exposed to transient cornering. On the grass surface, the tyres were able to generate sufficient lateral force to obtain understeer up to a maximum lateral acceleration of 0.6 g. Up to a maximum lateral acceleration of 0.35 g, the tyre grip level was still sufficient that the handling was stable on the grass and dirt track surfaces as compared to on the tarmac surface. On the dirt track surface, the tyre traction decreased at a lateral acceleration of 0.35 g and the vehicle exhibited oversteer at a maximum lateral acceleration of 0.39 g. The tyres were unable to develop sufficient lateral force on the dirt track surface for high lateral acceleration manoeuvres. When performing transient cornering, the ability of the tyres to develop a lateral force had the biggest influence on handling on surfaces which offered low tyre traction.

Contents

List of Figures

List of Tables

List of Symbols

The units of quantities defined by a symbol are indicated in square brackets following the description of the symbol. Quantities with no indicated units may be assumed to be dimensionless.

K Understeer gradient [deg/g].

L Vehicle wheelbase [m].

R Cornering radius [m].

V Voltage [V].

$\mathbf{r}$ Yaw rate [deg/s].

a CG distance from front axle [m].

a_y Lateral acceleration [g].

b CG distance from rear axle [m].

h CG height [m].

k Spring stiffness rate [N/m].

m Mass [kg].

n Vehicle gearbox ratio [–].

v_x Longitudinal velocity [m/s].

w Vehicle axle track width [m].

δ Steer angle [deg].

ϕ Roll angle [deg].

List of Acronyms

ADC analogue-to-digital converter.

ATV all terrain vehicle.

BMG Bearing Man Group.

CG centre of gravity.

CPR counts per revolution.

DAQ data acquisition.

DLC double lane change.

DOE design of experiments.

DOF degree of freedom.

FEA finite element analysis.

GPS global positioning system.

IMU inertial measurement unit.

MBD multibody dynamics.

ROV recreational off-highway vehicles.

SAE Society of Automotive Engineers.

UTV utility vehicle.

1 Introduction

The vehicle dynamics of on-road and off-road vehicles has been extensively studied, with the focus primarily being the handling capabilities of the vehicle, to achieve the optimal road holding capability and ride comfort. Numerous studies have focused on the design, modelling and optimisation of on-road vehicle suspensions, but the study of off-road vehicle dynamics is still relatively new. The aim of this dissertation is to analyse the differences in on-road and off-road vehicle handling. The dissertation aims to answer the following questions:

1. How does vehicle behaviour change over on-road and off-road terrain?
2. What effects do vehicle setup and tyre grip levels have on cornering stability and vehicle handling quality?

The Society of Automotive Engineers (SAE) runs an intercollegiate design competition known as the SAE Mini Baja competition, which involves the design, building and competing of an off-road vehicle for numerous objectives over harsh terrain [1]. The University of the Witwatersrand has competed in the SAE mini baja competition for many years. Figure 1.1 shows the 2014 Bearing Man Group (BMG) Wits mini baja vehicle.

The BMG Wits Baja will be the representative vehicle used to measure the accelerations and yaw rates during on-road and off-road vehicle handling tests. The differences in vehicle handling on on-road and off-road surfaces will be measured using the mini baja vehicle.

Figure 1.1: BMG Wits Baja vehicle 2014. [2]

1.1 Literature Review

Metz [3] measured the subjective and objective metrics for "good" handling. Metz argued that handling quality can be represented by three objective metrics, namely (1) resistance to rollover, (2) steady-state behaviour, and (3) transient behaviour. It was concluded that good handling qualities are exhibited by linear roll behaviour until rollover. In terms of steady-state handling, neutral steer up to the lateral acceleration limit is desirable for racing but if not possible, an understeer car would be favoured. For transient steering, such as step steering inputs, the time-domain yaw rate response is critical.

Brown et al. [4] examined the handling and control of a two-person recreational off-highway vehicles (ROV). The objective of the study was to investigate the directional control, and steering behaviour of an ROV with different handling configurations. The study examined steady-state handling characteristics of the vehicle during a circle-turn test similar to those set in SAE J266. The study was conducted on a dirt surface. An IMU was used to measure the pitch, roll and yaw angles and the vehicle accelerations. The steering angle, vehicle throttling and vehicle braking were also measured. All drivers preferred the "understeer transitioning to oversteer" vehicle setup, due to its manoeuvrability through the tighter corners. The "understeer" vehicle setup would experience yaw overshoot, due to the driver utilising a larger steering angle during cornering. Overall, the most favourable vehicle setup was one which transitioned to oversteer during cornering. It was concluded that, during off-road cornering, the vehicle experienced non-linear front and rear tyre saturation, which occurred at lateral accelerations much less than those performed on on-road terrain.

Renfroe et al. [5] examined the handling characteristics of an all terrain vehicle (ATV) and utility vehicle (UTV), then examined modifications to these vehicles to improve handling characteristics without substantial increases in cost. The tests were performed on a gravel surface. The steering angle, vehicle speed, and lateral acceleration were measured. It was found that the tuned ATVs and UTVs produced the most favourable handling results, producing neutral steer with slight understeer at higher lateral accelerations. It was shown that favourable handling could be achieved using cost-effective methods. This study demonstrated the importance of favourable vehicle handling for off-road surfaces

Pujatti et al. [6] presented a longitudinal performance test of a mini baja vehicle, to be validated by numerical models. The vehicle was instrumented to measure vehicle accelerations and velocities using an accelerometer, throttle and brake positions using a potentiometer, as well as transmission shaft angular velocity using an inductive sensor. The experiment, however, was only performed for longitudinal performance over a 100 m paved terrain. The results were overlayed, showing the exact instances of braking, throttling, vehicle acceleration and vehicle speed. The maximum achieved vehicle speed, acceleration and deceleration were 11.4 m/s, 1 g and 1.82 g respectively. Pujatti et al. demonstrated the use of measurement instruments for vehicle characterisation.

Kakria et al. [7] modelled a mini baja vehicle, using an integrated multibody dynamics (MBD) and finite element analysis (FEA) approach. An MBD model of the suspension system was built using ADAMS/Car, and using ADAMS/Insight, a design of experiments (DOE) was performed to minimise roll and camber during vertical wheel travel. Various tests, including double lane changes, constant radius cornering, sine input, steady-state and transient response tests were performed for the full vehicle model to predict the handling characteristics. The tests were modelled using flat paved roads. The camber angle and toe variation during wheel travel were reduced from $6°$ and $37°$ to less than $2°$ and $3°$ respectively. During the DLC test, the vehicle experienced a maximum lateral acceleration of 1.1 g. This study demonstrated the use of numerical modelling to improve vehicle handling.

Amaral et al. [8] studied the critical steering angle required for a lateral rollover on a mini baja vehicle. The proposed mathematical model was validated experimentally. The vehicle was fitted with a fifth lateral wheel, which would prevent a complete rollover, ensuring driver safety. The understeer gradient was determined for varying vehicle speeds and turn radii. The cornering stiffness of the tyres were estimated experimentally. The vehicle speed was measured using an encoder, positioned on the front wheel. The test was performed over flat paved road. The results showed that for low speeds, the critical steering angle remains constant for varying turn radii, since the lateral acceleration gain is more influenced by vehicle speed. At a vehicle speed of 11.4 m/s, and a turn radius of 14.3 m, the critical steering angle was determined to be 6.0°, producing a deviation between the mathematical model and experimental result of 10%. The primary cause of the difference was due to the inaccuracies of the estimated tyre model. Thus, understanding the effects of tyre stiffness is important in determining vehicle performance and overall safety.

Els [9] investigated the use of an active anti-roll bar to improve off-road vehicle handling, without sacrificing ride comfort. The proposed solution was simulated using ADAMS, and tested on a Land Rover Defender 10. The results indicated that the anti-roll bar successfully reduced body roll up to a 0.4 g lateral acceleration limit. At a vehicle speed of 19.44 m/s, the body roll was significantly reduced by between 40% and 74% during dynamic handling. This study demonstrated the importance of vehicle stiffness on the overall handling quality. The anti-roll bar allowed the tyres to maintain a larger contact area with the ground, improving road holding capability.

Pytka et al. [10] instrumented a vehicle for dynamics testing on off-road conditions. The purpose was to show how a vehicle could perform vehicle tests without special modifications (rather the addition of measurement instruments only). Tests were conducted on a Suzuki Vitara and instrumentation included four strain gauge type wheel force sensors, a steering angle sensor and robot, a differential GPS system, a vehicle speed sensor, and a computer to perform tests and log data. The instrumented vehicle was capable of measuring wheel forces and moments, vehicle speed, and vehicle body accelerations.

Katzourakis et al. [11] instrumented a race-car for vehicle dynamics testing. A draw-wire potentiometer was used to measure the steering angle at the steering wheel. The angular velocity of each wheel was measured using an optical encoder mounted to custom-designed hubs. The vehicle's position and slip angle was measured using a VBOX IISL utilising GPS signals. The vehicle accelerations as well as rotation rates were measured using a five degree of freedom (DOF) IMU. This allowed measurement of longitudinal, lateral and vertical accelerations, as well as the pitch and yaw rate. Brake pressure sensors were placed on both the front and rear hydraulic lines to measure braking pressure, position and duration. The throttle position was measured using a potentiometer connected to the bowden cable at the intake manifold. The data logging was performed by a compact notebook and a National Instruments NI USB-6211 DAQ, powered by a 12 V DC battery. A constant radius test was conducted over a loose gravel surface. The maximum lateral acceleration, yaw rate and a sideslip angle were 0.5 g, 35 deg/s and 40 deg respectively. The measured throttle and braking gave further insight into the reactive control of the vehicle by the driver, and how driver skill influenced vehicle handing.

Stewart et al. [12] investigated the study of rollover, lateral handling and obstacle avoidance manoeuvres of tactical vehicles for military use. The vehicle used was a standard Jeep and an "armoured" Jeep, which incorporated added mass. The rollover simulation indicated a lateral rollover of 1.16 g and 0.94 g for the standard and armoured vehicle respectively; a difference of 19.2%. The obstacle avoidance manoeuvre was simplified to a step steering input. At a vehicle speed of 22.4 m/s, the standard vehicle model indicated an unstable steering condition, as the side-sip angle achieved was 55°, indicating dangerous oversteer. The model also showed a maximum lateral acceleration of 0.6 g. The armoured vehicle indicated unstable steering conditions at a vehicle speed of 18.3 m/s, corresponding to maximum lateral acceleration of 0.4 g.

In summary, a detailed review of the following literature has been presented:

- SAE standards for vehicle cornering tests [4, 5].
- The analytical model of the critical steering angle to induce lateral rollover [8].
- Numerical modelling using multiple modelling software such as MSC ADAMS [13, 9].
- Methods for instrumentation of a vehicle for both on and off-road handling tests [14, 6, 4, 13, 9, 10, 11].
- Measurement instruments for use in vehicle dynamics testing [6, 10, 11]
- Suspension configurations for a mini baja vehicle [7].
- Suspension designs of non-baja vehicles (passive type, semi-active type, and active type) to optimise road holding and ride comfort characteristics [9].
- Suitable methods for analysis of vehicle ride comfort and vibration level for both on-road and off-road surfaces [14].
- Comparative results for mini baja vehicle handing tests [6, 7, 8].
- Objective metrics to describe vehicle handling [3].
- The effect of inertial properties on rollover and obstacle avoidance [12].

Figure 1.2 shows the existing literature for vehicle handling tests subjected to steady-state and transient steering. To the author's knowledge there exists only a single study [10], which has performed vehicle handling tests off-road. The vehicle used was not a mini baja vehicle. Vehicle handling tests have only been performed (either by experimental or numerical methods) on paved, straight roads. Although Renfroe et al. [5] performed test on gravel, this test was only performed on ATV type vehicles.

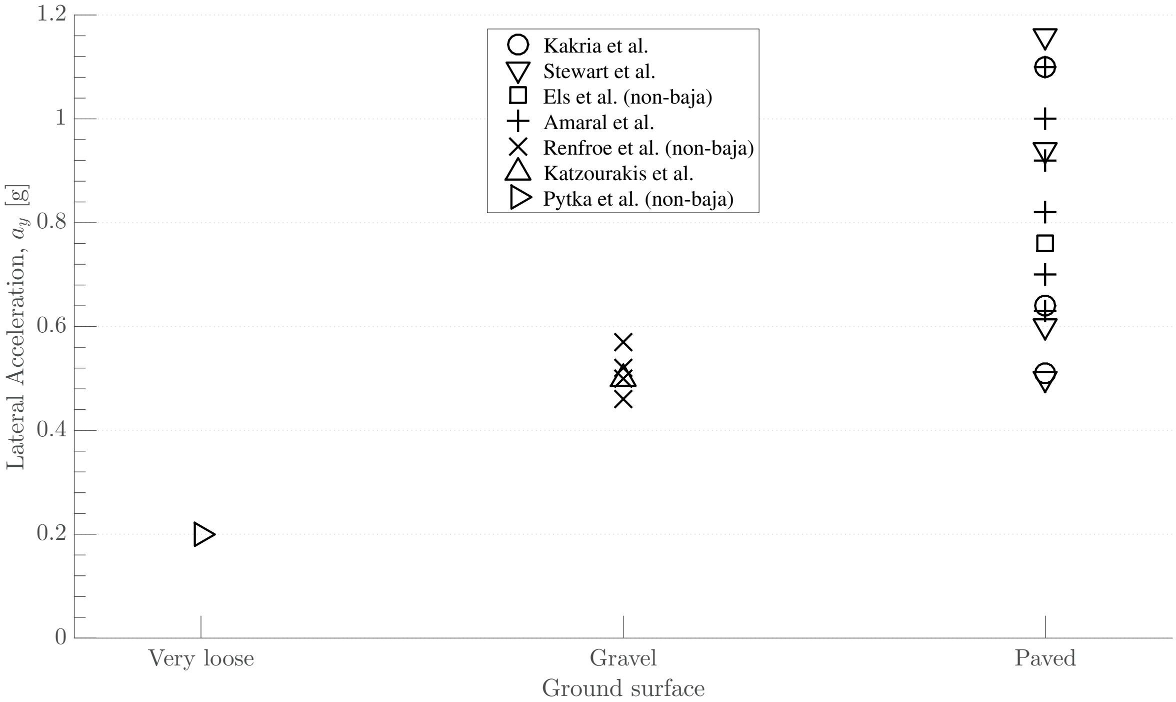

Figure 1.2: Review of existing vehicle handling tests.

Figure 1.3 shows the existing literature for vehicle handling tests, performed by either experimental or numerical methods. Little research has been conducted off-road on a mini baja vehicle. Although Owens et al. [15] investigated the loading conditions typically experienced on off-road terrain and over obstacles, the scope of that study did not encompass the vehicle handling aspect (merely load characterisation for design purposes). There exists a research gap for a better understanding of off-road vehicle handling.

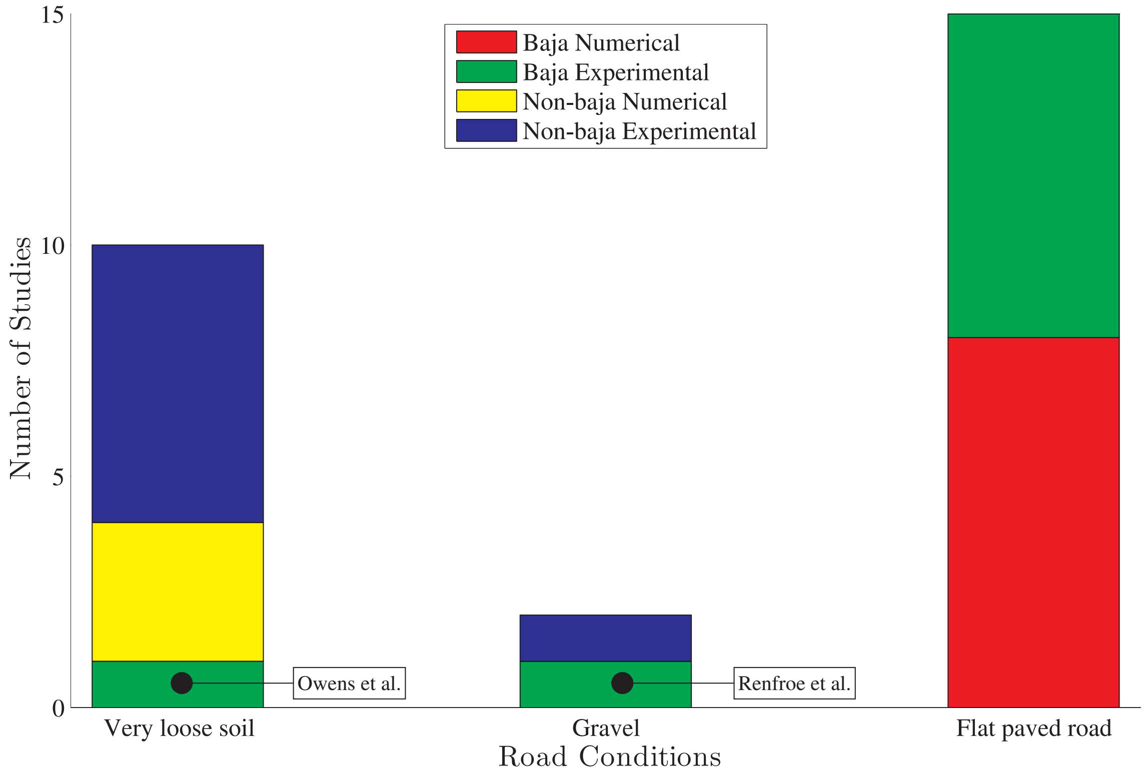

Figure 1.3: Review of existing experimental and numerical literature.

1.2 Motivation and Significance of the Study

The literature detailed in Section 1.1 above shows that there exists a gap in the study of off-road handling of a mini baja vehicle. To the authors knowledge, the only available studies on handling dynamics for mini baja vehicles were performed on-road. It is still not yet fully understood how a mini baja vehicle handling varies during off-road cornering compared to on-road.

The significance of this study is to not only to perform off-road tests, but to quantitatively describe the differences between off-road and on-road vehicle handling for a mini baja vehicle. By understanding on-road and off-road differences, it will be possible to relate on-road numerical models to "real" off-road terrain. This study will aid in determining the best vehicle setup and design for off-road use.

1.3 Objectives

The objectives of this dissertation are as follows:

1. Characterise the steady-state cornering performance of a mini baja vehicle for on-road and off-road surfaces.
2. Evaluate the closed-loop mini baja vehicle response using the DLC manoeuvre, for on-road and off-road surfaces.
3. Evaluate the open-loop mini baja vehicle response using the step steering input manoeuvre, for on-road and off-road surfaces.

2 Background

2.1 Vehicle Dynamics

This chapter details background theory and equations to describe vehicle body motion, and methods to determine vehicle handling performance.

For the purpose of analysis, it is convenient to represent a vehicle by using the "bicycle model" as shown in Figure 2.1. This numerical model includes the effects of fornt and rear tire cornering stiffness, location of the centre of gravity (CG), wheelbase and steer angle on the vehicle yaw and sideslip motion. [16], [17]

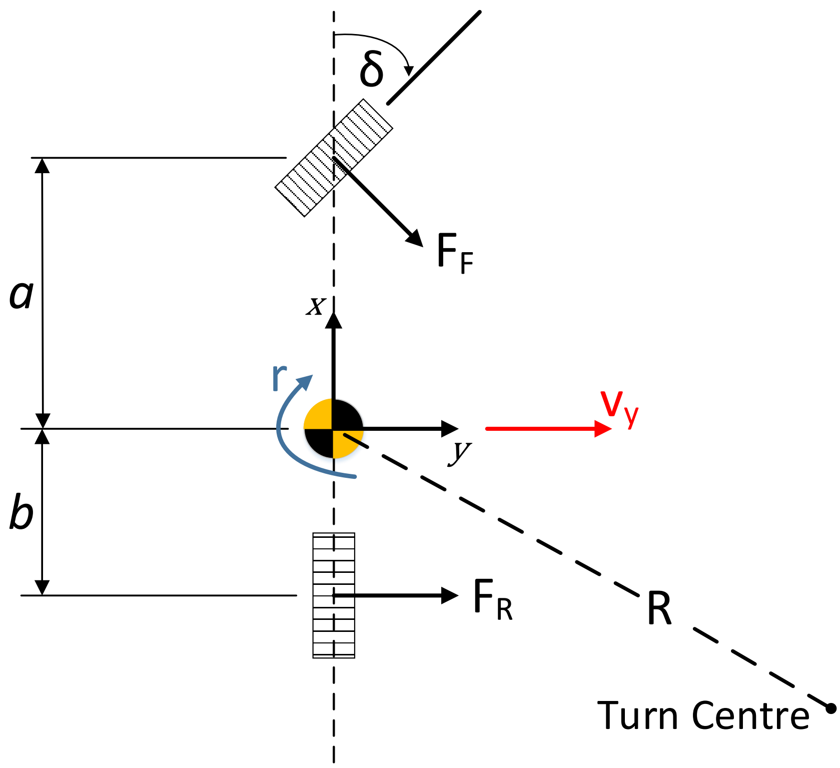

Figure 2.1: The bicycle model.

If a constant longtiudinal acceleration is assumed, the steady state cornering equation is derived from Newton's second law and is defined as follows [17]:

$$\delta = \frac{L}{R} + \left(\frac{W_F}{C_{\alpha F}} - \frac{W_R}{C_{\alpha M}} \right) \frac{v_x^2}{gR} \tag{2.1}$$

Where δ is the steering input applied by the driver in deg, L is the vehicle wheelbase in m, R is the turn radius of the vehicle in m, W_F and W_R are the vehicle loads over the front and rear axles respectively in N, v_x is the vehicle speed in m/s, $C_{\alpha F}$ and $C_{\alpha R}$ are the cornering stiffness' of the front and rear tires respectively in N/deg, and g is the gravitational constant in m/s^2.

The equation for steady state cornering is often described in shorthand as follows:

$$\delta = \frac{L}{R} + Ka_y \tag{2.2}$$

Where K denotes the understeer gradient in deg/g, and a_y is the lateral acceleration of the vehicle in g.

The understeer gradient describes the cornering behaviour of a vehicle for any turn radius R, and is a useful metric for describing handling performance. Three possibilities of understeer gradient exist:

1. $K = 0$ (Neutral steer):
   For a constant radius turn, no change in steer angle will be required as the vehicle speed is increased.

2. $K < 0$ (Understeer):
   For a constant radius turn, the steer angle will have to increase for increasing vehicle speed.

3. $K > 0$ (Oversteer):
   For a constant radius turn, the steer angle will have to decrease for increasing vehicle speed.

The understeer gradient varies depending on the vehicle velocity, lateral acceleration and the friction level between the tires and the surface. Thus a local derivative must be determined [17]. It is possible to determine the understeer gradient of a vehicle through experimental methods. The understeer gradient of a vehicle is represented through the use of a "cornering diagram". Understeer is measured by cornering the vehicle under constant radius turn and observing the steering angle input, versus lateral acceleration output [17].

Given the radius of turn R and vehicle speed V, the lateral acceleration and yaw rate is determined as follows:

$$\begin{aligned} a_y &= \frac{v_x^2}{Rg} \\ \mathbf{r} &= \frac{a_y}{v_x} \end{aligned} \tag{2.3}$$

Figure 2.2 shows the typical handling characteristics for a neutral steer, understeer and oversteer vehicle operating at constant speed over varying turn radii [17].

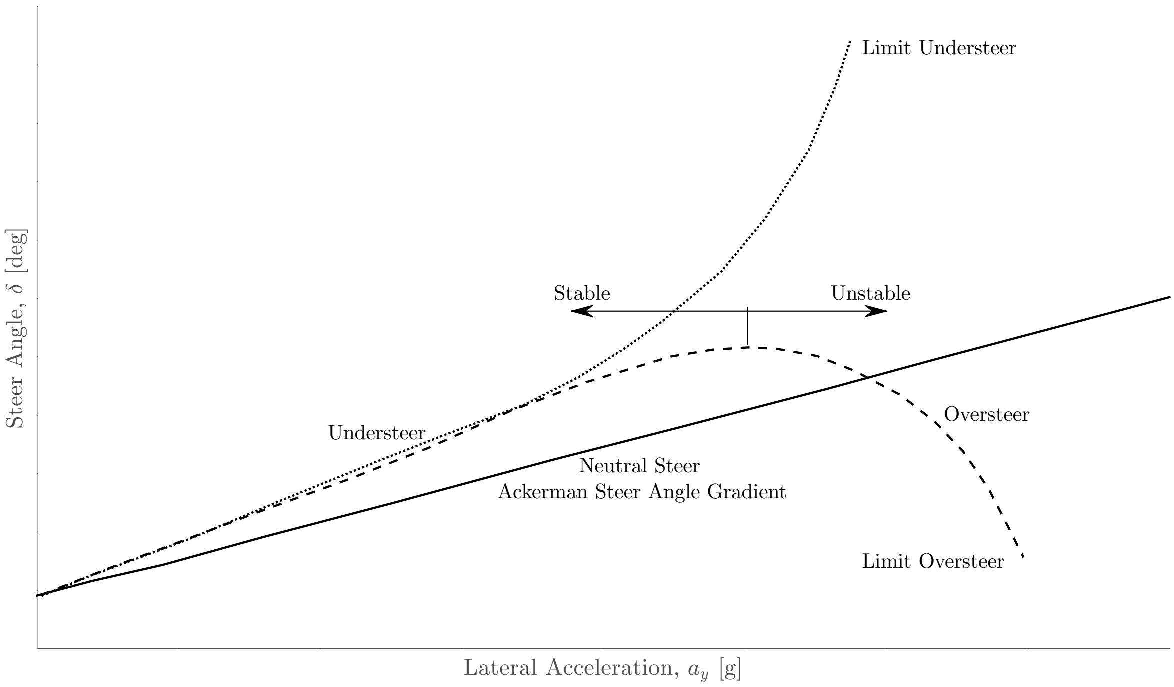

Figure 2.2: Understeer gradients for a neutral steer, understeer and oversteer vehicle.

A significant point on the handling diagram is the lateral force at which vehicle handling changes from understeer to oversteer. This can have serious detrimental effects on vehicle handling and controllability. Any point where the local gradient is above the neutral steer line indicates vehicle understeer. Conversely, any point where the local gradient is below the neutral steer line indicates vehicle oversteer. The lateral forces developed by the tires play are the dominant role in the determination of the handling diagram.

During low-speed cornering the tires do not need to develop a lateral force to counteract the force due to lateral acceleration. Under cornering conditions in which the tire develops a lateral force, the tire also experiences lateral slip, α as it rolls [17]. Figure 2.3 shows a typical cornering force diagram for a tire. The distinct operating regions are also shown.

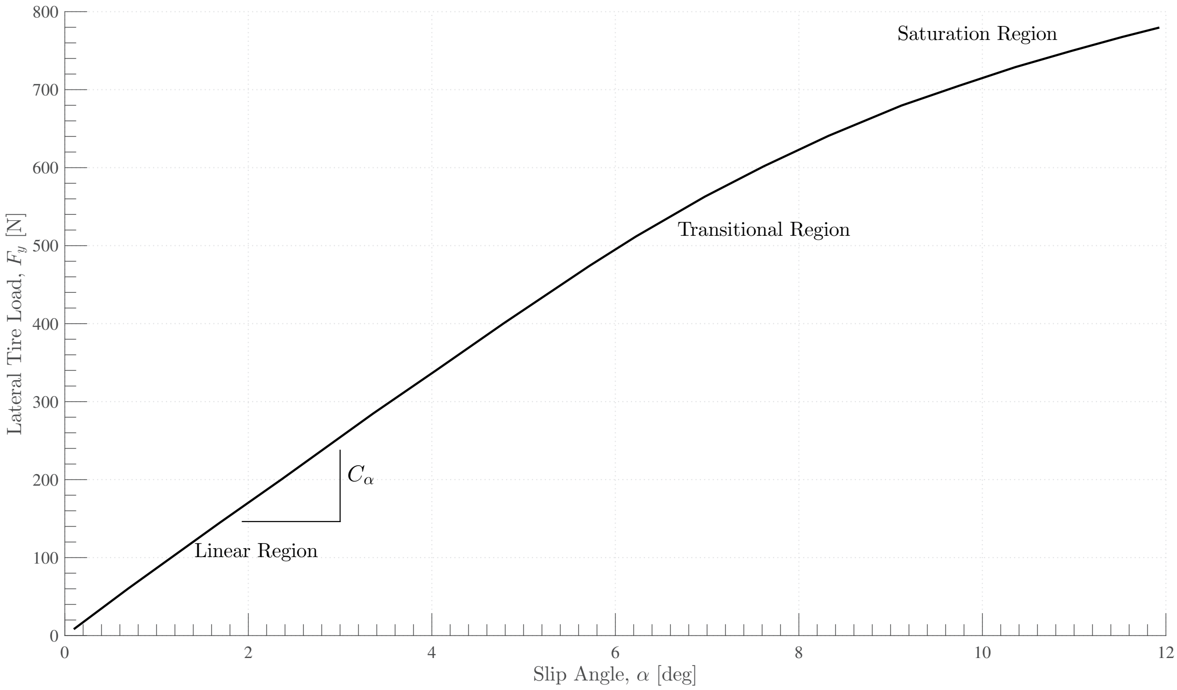

Figure 2.3: Tire cornering stiffness curve. [17]

At low slip angles, the tire develops a linear lateral acceleration with increasing slip angle. The proportional constant, C_y is the cornering stiffness in N/deg. At higher slip angles, the ability of the tire to develop the required lateral force decreases and the tire is said to be "saturated". The point at which tire saturation occurs has been shown to directly affect cornering performance. The cornering stiffness of a tire is dependent on many variables, including tire load, inflation pressure and road surface.

2.2 BMG Wits Baja Vehicle

The vehicle inertial, geometric and suspension parameters of the BMG Wits Baja vehicle are outlined in Table 2.1.

Table 2.1: BMG Wits Baja vehicle parameters.

Parameter		Unit	Value
Inertial properties	Total Mass, m	kg	266
	Yaw moment of inertia, I_{zz}	kgm^2	93
Geometric properties	Wheelbase, L	mm	1497
	Front axle track width, w_f	mm	1194
	Rear axle track width, w_r	mm	1015
	CG distance from front axle, a	mm	898
	CG distance from rear axle, b	mm	599
	CG height, h	mm	615
Suspension properties	Spring stiffness, k	N/mm	18
Gearbox properties	Gearbox ratio, n	–	0.1122

2.3 Steady State Cornering According to ISO 4138

The steady state circular test manoeuvre assesses the steady state cornering ability of the vehicle, and its understeer behaviour through increasing lateral acceleration. There exists three methods to measure the steady state cornering behaviour outlined in ISO4138, namely [18]

1. **Constant radius** method, where the cornering radius is maintained constant whilst vehicle speed is increased and steering controlled,
2. **Constant steering wheel angle** method, where the steering wheel angle is maintained constant whilst vehicle speed is increased, and
3. **Constant speed** method, where the vehicle speed is maintained constant whilst steering is incremented.

For this test, the following outputs are measured:

1. **Longitudinal velocity**, v_x in m/s,

2. **Lateral acceleration**, a_y in g,

3. **Cornering radius**, R in m,

4. **Steering wheel angle**, δ in degrees,

5. **Roll angle**, ϕ in degrees, and

6. **Yaw rate**, **r** in deg/s.

2.4 Step Steering Input According to ISO 7401

The step input steering test is an open-loop manoeuvre which assesses the transverse dynamic behaviour of a vehicle. The objectives of this test are as follows:

1. Determine the time-shift between steer angle, lateral acceleration and yaw rate in the time domain,

2. Determine the yaw rate gain in the time domain, and

3. Determine the lateral acceleration and yaw rate response to steering angle in the frequency domain.

For this test, the following outputs are measured:

1. **Longitudinal velocity** v_x in m/s,

2. **Lateral acceleration** a_y in g,

3. **Cornering radius** R in m,

4. **Steering wheel angle** δ in degrees,

5. **Roll angle** ϕ in degrees, and

6. **Yaw rate r** in deg/s.

Figure 2.4 depicts the test setup used.

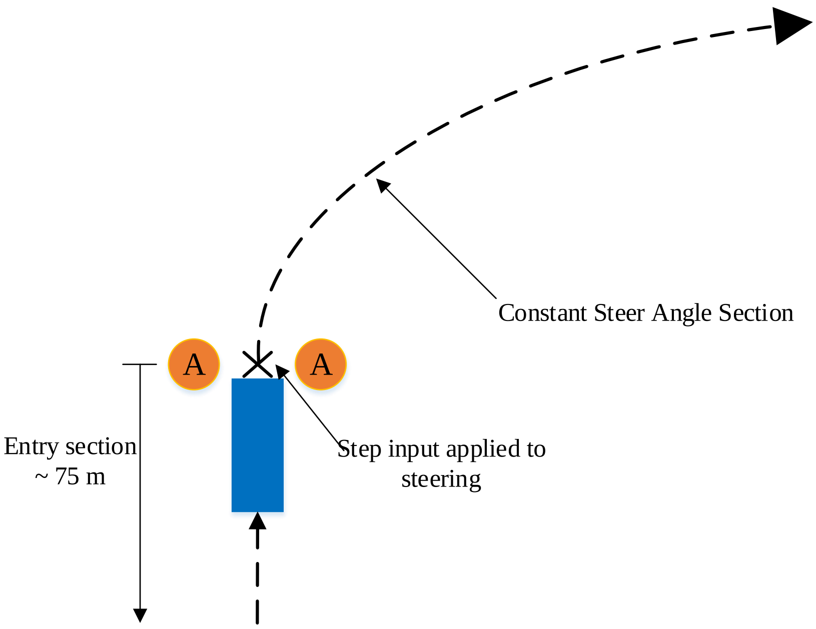

Figure 2.4: ISO 7401 step steer input test. [19]

2.5 Transient Cornering According to ISO 3888

The DLC test is a closed-loop manoeuvre which assesses the transient cornering ability of the vehicle, and its time domain response to sudden steering input [20]. The manoeuvre is depicted in Figure 2.5. The manoeuvre consists of an entry, side and exit lane. The vehicle speed must be measured at points A and B (indicated by the blue lines).

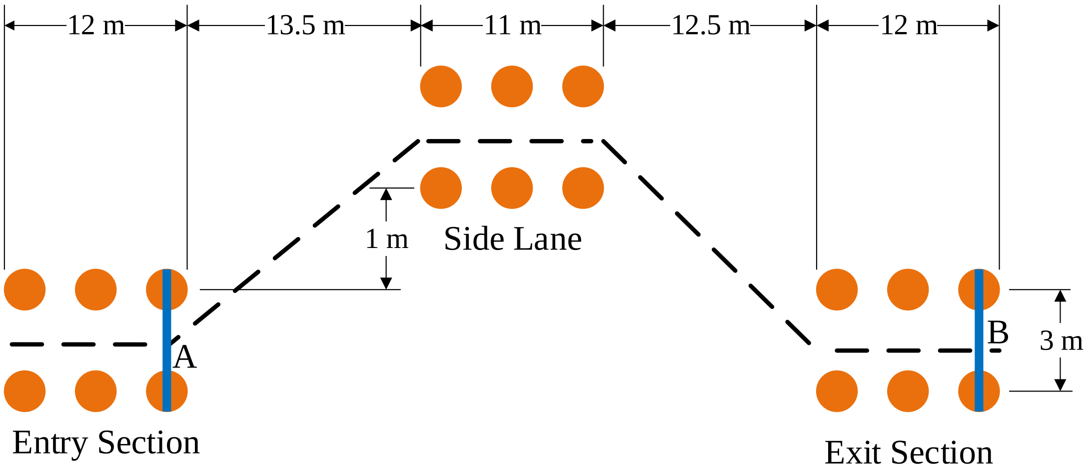

Figure 2.5: ISO 3888 DLC testing track. [20]

For this test, the following outputs are measured:

1. **Longitudinal velocity** v_x in m/s,
2. **Lateral acceleration** a_y in g,
3. **Steering wheel angle** δ in degrees,
4. **Roll angle** ϕ in degrees, and
5. **Yaw rate r** in deg/s.

3 Experimentation

This chapter details the experimental procedures followed for the vehicle handling experimental methodology.

3.1 Instrumentation

It was required to assess the vehicle handling of the mini baja vehicle. This required the measurement of the vehicle accelerations, steer angle, brake position and throttle position during cornering manoeuvres. The following instrumentation were used for the vehicle handling tests:

- An IMU to measure linear accelerations and angular rates of the vehicle.
- A steering sensor to measure the steer angle.
- A throttle sensor to measure the position of the throttle.
- A brake sensor to measure the position of the brake.
- A wheel speed sensor to measure the wheel rotational speed.
- A data acquisition (DAQ) system to log and store the data.

Accelerometers were used to determine vehicle accelerations. Gyroscopes were used to determine the pitch, yaw and roll motion. The position of the throttle and brake were measured using draw-wire potentiometers. An encoder was used to measure rear wheel angular velocity. Table 3.1 summarises the measurement instruments used for the dynamic handling tests.

Figure 3.1 shows the test vehicle used for the vehicle handling tests.

Figure 3.2 shows the wiring schematic used.

Table 3.1: Instrumentation used for dynamic handling tests.

Micro-controller	Brand:	Arduino Mega R3
	Additional shield	Adafruit Data Logger Shield
	Input power:	6–20 V
	Analogue resolution:	4.89 mV
	Sampling rate:	20 Hz
IMU	Brand:	Sparkfun LSM9DS0
	Input power:	2.4–3.6 V
	Accelerometer range:	$\pm$ 2, 4, 6 or 8 g
	Gyroscope range:	$\pm$ 245, 500 or 2000 °/s
	Magnetic field range:	$\pm$ 2, 4, 8 or 12 guass
	Accelerometer resolution:	0.01 m/s^2
	Gyroscope resolution:	0.01 deg/s
	Interface:	I2C
Throttle Sensor Brake Sensor	Brand:	Micro-Epsilon WPS-MK30
	Measurement range:	250 mm
	Sensor element:	Potentiometer
	Resolution:	$\pm$ 0.1 mm
Steer Angle Sensor	Brand:	Micro-Epsilon WPS-MK-30
	Measurement range:	750 mm
	Sensor element:	Potentiometer
	Resolution:	$\pm$ 0.2 mm
Wheel Speed Sensor	Brand:	Avago Technologies
	Encoder type:	Incremental Magnetic
	Input power:	4.5–5.0 V
	Resolution:	256 counts per revolution (CPR)
	Output waveform:	50% duty cycle square wave
	Rated rotational speed:	7000 RPM
Stopwatch Timer	Resolution:	0.1 s

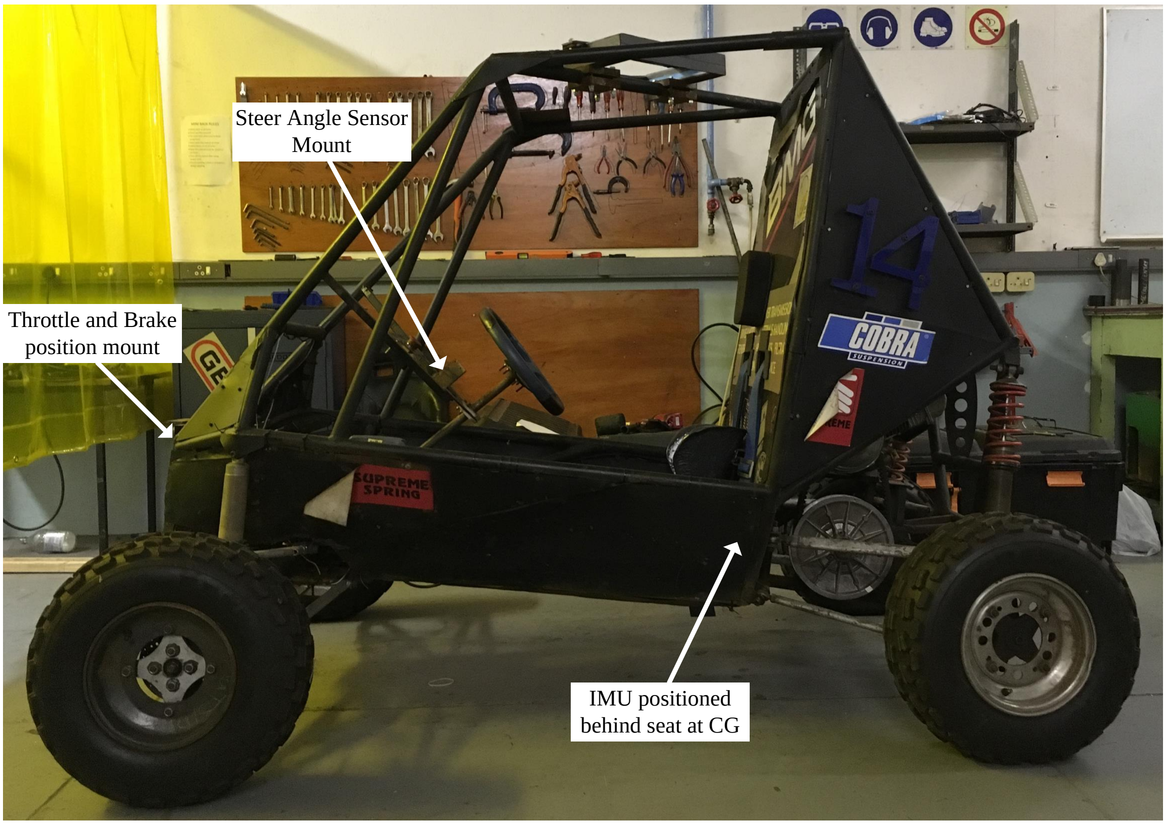

Figure 3.1: Test vehicle used for handling tests.

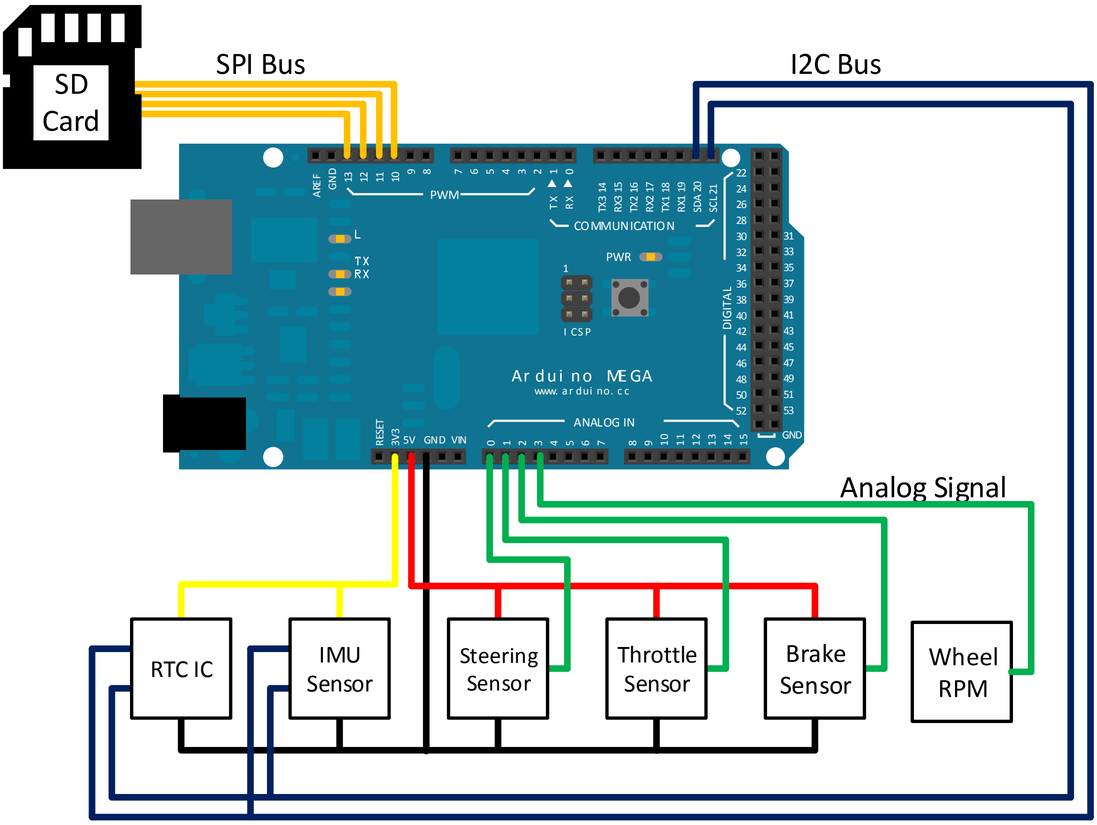

Figure 3.2: Instrumentation wiring schematic.

3.2 Calibration

3.2.1 Steering Angle Sensor Calibration

The steering angle sensor was placed on a mounting bracket welded to the chassis and the draw-wire was looped around the steering column. The steering angle sensor required calibration to accurately determine the position of the front wheels relative to the steering input. The BMG Wits Baja closely approximates an Ackerman steering, and thus the cot-average of the inner and outer front wheels were used to obtain the steer angle. The equation is defined as [17]:

$$\cot\delta = \frac{\cot\delta_L + \cot\delta_R}{2} \tag{3.1}$$

Where δ is the steer angle in deg, δ_L is the steer angle of the left-front wheel in deg and δ_R is the steer angle of the right-front wheel in deg. The calibration curve is shown in Figure 3.3. The output of the steer angle sensor was compared to the measured steer angles of each wheel. The calibration curve was defined as follows:

$$\delta = -108.4492V + 266.7593 \tag{3.2}$$

Where δ is the vehicle steer angle in deg and V is the measured analogue voltage in V.

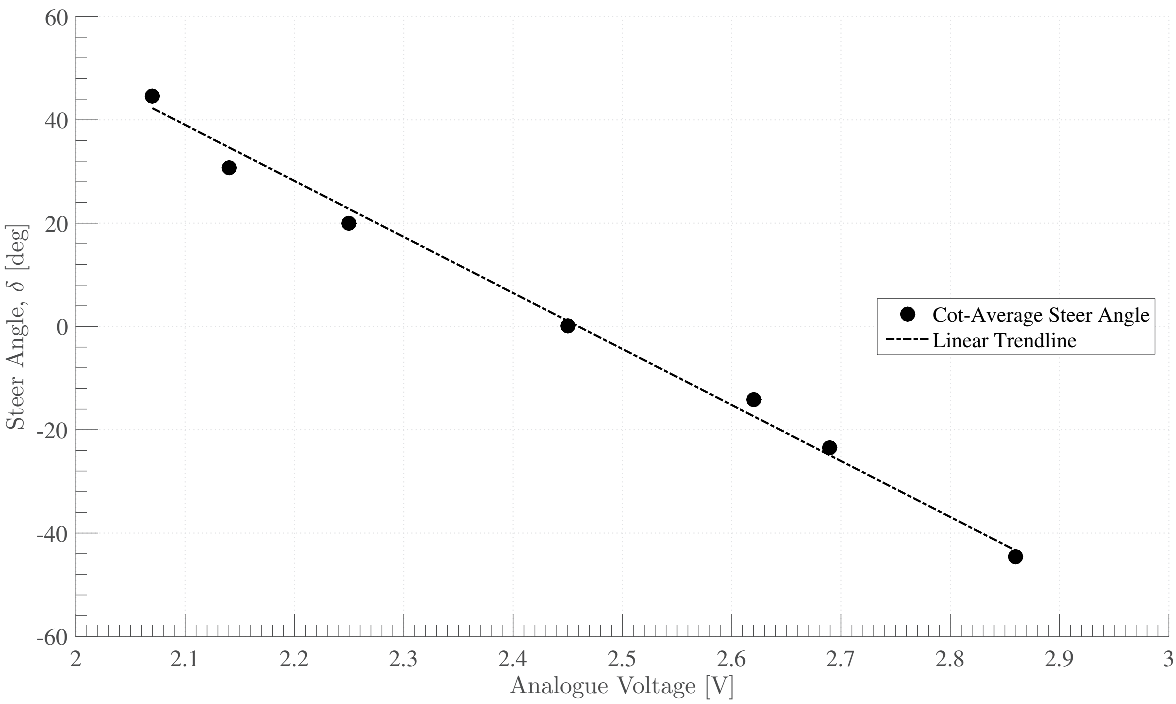

Figure 3.3: Steer angle calibration curve.

3.2.2 Accelerometer Calibration

The IMU was placed in a protective housing to protect the circuitry from dirt, moisture and shock. All three axes of the accelerometer were tested relative to gravity. A jig was used to hold the accelerometer in all three axes relative to gravity. The process was repeated twice to verify that no drift occurred over a time interval of 6 hours under constant operation. The averaged results are given in Table 3.2.

Table 3.2: Accelerometer calibration values relative to gravity.

	Exposed to +1 g	Exposed to -1 g
X Axis	1.02	-1.01
Y Axis	0.99	-1.03
Z Axis	1.00	-0.97

3.3 Vehicle Test Setups

3.3.1 Steady-State Cornering

The constant speed method (refer to the methodology of ISO 4138 in Section 2.3) was performed to evaluate the steady-state steering and handling response. The test setup was as follows:

- The longitudinal velocity of the vehicle was maintained constant,
- The vehicle turn radius was incrementally reduced so as to increase the lateral acceleration, and
- The steer angle was varied to perform the required turn manoeuvre.
- Steady-state conditions were fulfilled when the driver did not have to correct the steering angle during the turn.

The test was performed at the maximum speed of the vehicle ($\approx$ 5 m/s), since the steering characteristics at larger lateral accelerations are of greater interest for racing purposes. The driver had to make the steering corrections to maintain the turn radius and ensure that steady-state conditions had been reached.

3.3.2 Step Steering Test

A simple step steering input test (refer to the methodology of ISO 7401 in Section 2.4 above) is used to examine the open-loop vehicle controllability. The test setup was as follows:

1. The longitudinal velocity was maintained constant,
2. The steer angle was sharply increased to input a step, and was held against a mechanical stop, and
3. The driver would maintain the speed and steer angle until quasi-steady-state results were achieved.

3.3.3 Double Lane Change

A DLC test was performed at a constant longitudinal velocity to evaluate the effect of transient steering on closed-loop vehicle handling. The ISO 3888 test setup was adjusted as shown in Figure 3.4. The reasons the standardised setup was changed were as follows:

- The baja cannot attain the same speeds as that used by ordinary motor vehicles, i.e. higher than 50 km/h, and
- The baja has a much smaller wheelbase and track as compared to ordinary motor vehicles, and as such has a smaller turn radius

Due to the much lower vehicle speeds and smaller turning radius, the course would have to incorporate higher turn radii in order to experience larger lateral acceleration and yaw rates. This is required in order to evaluate vehicle handling performance. The average longitudinal velocity achieved through the test section was measured using a stopwatch – by measuring the time required to travel a set distance – to measure the average longitudinal velocity at points A and B respectively.

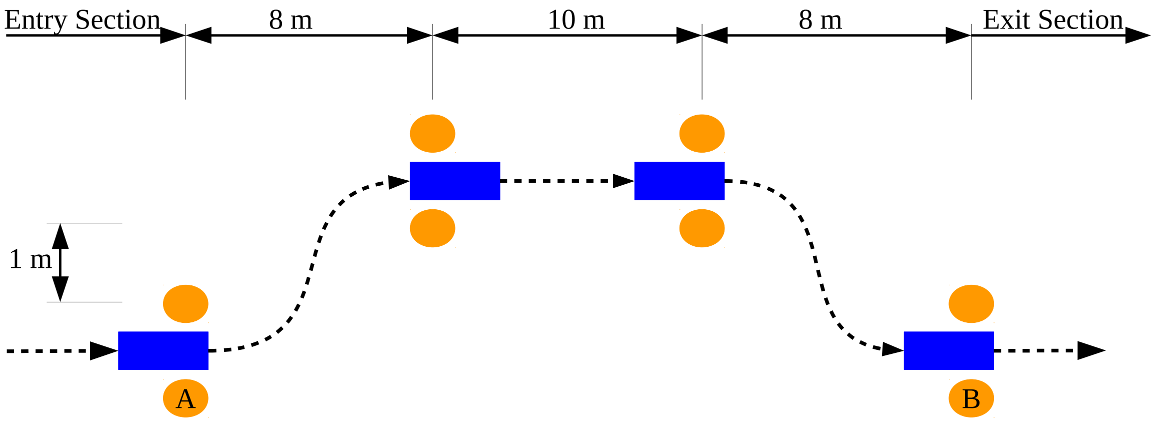

Figure 3.4: ISO 3888 DLC manoeuvre used for testing.

3.3.4 Road Conditions

To characterise off-road handling, the road conditions must be specified. All tests were performed on various road condition types. The purpose of this was to evaluate the vehicle handling with respect to different tire grip levels. The surface conditions were as follows, and are detailed in Figures 3.5 to 3.7.

1. A tarmac surface would be used as a control test condition, with high tire grip levels,
2. A grass field surface would offer intermediate tire grip levels, and
3. A dirt track surface would offer poor tire grip levels.

Figure 3.5: Tarmac road condition used for testing.

The surfaces were selected such that vertical motion was reduced as much as possible. The tarmac surface was relatively flat, but the grass field and dirt track surfaces had unavoidable

Figure 3.6: Grass field surface condition used for testing.

Figure 3.7: Dirt track surface condition used for testing.

deviations in the surface. This was deemed acceptable for testing as a baja vehicle is specifically designed for off-road use.

3.4 Procedure

The following procedure was used for each surface for the handling tests:

1. The route markers were set up according to the required steady-state cornering track, DLC or step steering input test.
2. The vehicle was placed at the start of the entry section, which was approximately more than 50 m away from the "test section". This would allow the driver to accelerate up to a maximum velocity and maintain the longitudinal velocity through the "test section".
3. The driver would accelerate up to the vehicle's maximum velocity and perform the manoeuvre according to the marker setup.
4. Once the manoeuvre was completed the driver would bring the vehicle to a complete stop.

3.5 Precautions

The following precautions were pertinent to the quality of the observations of the dynamic experiment:

1. A measuring tape was used to ensure the route markers were accurately positioned.
2. The calibration of the steering angle sensor was performed on level ground to eliminate the effects of wheel camber on steering angle.
3. The same driver was used for every test so as not to introduce variation in vehicle handling due to driving style.
4. The driver was allowed test runs over the course before performing the vehicle tests. This allowed the driver to become accustomed to the vehicle behaviour over the varying terrain. This would reduce the variation in the test data due to the driver slowly learning to anticipate the vehicle behaviour.
5. A total of nine experiments were performed for each manoeuvre. An average of these results would reduce anomalies due to driver influence.
6. The throttle was maintained constant at its maximum to ensure maximum vehicle speed throughout the test sections.

3.6 Possible Risks and Countermeasures

The following measures were taken in order to ensure the safety of both the driver and the partner responsible for starting the vehicle:

1. The driver wore all safety equipment required for racing; these included a helmet, fire-retardant overalls and gloves, as well as safety boots.
2. The driver assembled the five-point harness of the vehicle prior to every test run. This would ensure driver safety in the event of a rollover or crash.
3. The wiring harness used to connect each sensor was secured to the chassis out of the way of the driver to ensure it would not obstruct driver visibility.
4. Two kill switches were installed on the vehicle to allow a quick shut down of the engine in the case of danger; one for the driver inside the vehicle, and one for the partner on the outside of the vehicle.
5. The partner would evacuate the area behind the vehicle once the engine was started. The driver would not begin until the area was vacated.

4 Data Processing

This chapter details the formulae used to process the data from the experimental testing.

4.1 Formulae Used

4.1.1 Reading and Conversion of Raw Data

The IMU outputs the acceleration and yaw rate data in m/s^2 and deg/s respectively. the lateral acceleration were converted from m/s^2 to g using the following:

$$a_y\,[\text{in g}] = \frac{a_y\left[\text{in m/s}^2\right]}{9.80665}$$

Where 9.80665 is the standard acceleration due to gravity. The yaw rate was left in deg/s.

The steer angle was determined using the calibration equation:

$$\delta = -108.4492V + 266.7593$$

Where V is the measured output voltage from the draw-wire potentiometer in V.

4.1.2 Determining Steady State Conditions

To determine when the vehicle reached steady state the derivative of the steer angle time history was performed. A linear discretisation was performed using a forward differences method between time steps. A tolerance of 1e^{-3} was used to satisfy the discretisation.

$$\frac{d\delta}{dt} \approx \frac{\delta_{t+\Delta t} - \delta_t}{\Delta t} < 1\text{e}^{-3}\ \text{deg/s}$$

The values of the steady-state steer angle, lateral acceleration, and yaw rate were calculated from the average values during steady state conditions.

The understeer gradient was determined as follows:

$$K = \frac{\partial \delta}{\partial a_y} \\ = \frac{\delta_S}{a_{y,S}} \tag{4.1}$$

Where K is the understeer gradient in deg/g, δ_S is the steady state steer angle in degrees and $a_{y,S}$ is the steady-state lateral acceleration in g.

The yaw rate gain of the step-steer input tests were calculated as follows:

$$G_{\mathbf{r}} = \frac{\partial \mathbf{r}}{\partial \delta} \\ = \frac{\mathbf{r}_S}{\delta_S} \tag{4.2}$$

Where $G_{\mathbf{r}}$ is the yaw rate gain in s^{-1} and $\mathbf{r}_S$ is the steady state yaw rate in deg/s.

4.1.3 Determining the Maxima and Minima of the DLC Manoeuvre

The maximae and minimae of the time-history data for the DLC manoeuvre was determined using the `findpeaks` function within MATLAB. The indices of the maxima and minima of the transient steer angle were used to calculate the maxima and minima for the lateral acceleration and yaw rate.

The standard deviation of the maximae and minimae were calculated as follows:

$$\sigma = \sqrt{\frac{\sum_{i=1}^{N} (x - \bar{x})^2}{N - 1}}$$

Where $N = 9$ samples were used.

4.2 Uncertainty Analysis

The total uncertainty of all dependent variables were assumed to have a linear behaviour at the measurement point, i.e.:

$$\frac{\Delta f}{f} \approx \frac{1}{f}\sum_{i=1}^{N}\frac{\partial f}{\partial x_i}dx_i$$

The uncertainty of the measurement of the analogue steer value was calculated as follows. The input power to the steer angle was assumed constant at 5 V as the power from the data logger was controlled by a switching voltage regulator to ensure a clean signal input. The micro-controller used a 10-bit analogue-to-digital converter (ADC).

$$\begin{aligned}\Delta \text{V} &= \frac{5\ \text{V}}{2^{10}}\\ &= \frac{5}{1024}\\ \therefore \Delta\delta &= 4.89\ \text{mV}\end{aligned}$$

The uncertainty of the calibration curve due to the analog measurement is as follows:

$$\begin{aligned}\Delta\delta &\approx \frac{\partial\delta}{\partial \text{V}}\Delta \text{V}\\ &= -108.4492\Delta \text{V}\\ \therefore \Delta\delta &= -0.053\text{deg}\end{aligned}$$

The uncertainty of the measurement of the steer angle during calibration was ± 0.5 deg. This uncertainty was assumed as the dominant factor in the total uncertainty of the steer angle measurement, i.e. $\Delta\delta \approx 0.5$ deg.

The uncertainty of the lateral acceleration (in g), was determined as follows, from the resolution of the measurement from the data logger, i.e. $\Delta a_y = 0.01\ \text{m/s}^2$:

$$\begin{aligned}\Delta a_y &= \frac{0.01}{9.80665}\\ \therefore \Delta a_y &= 0.001\ \text{g}\end{aligned}$$

The uncertainty of the understeer gradient was determined using Equation 4.1:

$$\begin{aligned}\Delta K &\approx \frac{\partial K}{\partial\delta}\Delta\delta + \frac{\partial K}{\partial a_y}\Delta a_y\\ \therefore \Delta K &= \left(\frac{1}{a_y}\right)\Delta\delta + \left(-\frac{\delta}{a_y^2}\right)\Delta a_y\end{aligned}$$

The total uncertainty of the understeer gradient is outlined in Table 4.1.

Table 4.1: Total calculated uncertainty using linear approximations.

Parameter	Unit	Nominal Value	Bias Value
δ	deg	11.32	0.5
a_y	g	0.274	0.001
K	deg/g	41.31	1.67

The uncertainty of the yaw rate was simply the resolution of the measurement of the yaw rate from the data logger, i.e. $\Delta\mathbf{r} = 0.01$ deg/s.

The uncertainty of the yaw rate gain was determined using Equation 4.2:

$$\begin{aligned}\Delta G_{\mathbf{r}} &\approx \frac{\partial G_{\mathbf{r}}}{\partial \mathbf{r}} d\mathbf{r} + \frac{\partial G_{\mathbf{r}}}{\partial \delta} d\delta \\ &= \left(\frac{1}{\delta}\right) \Delta\mathbf{r} + \left(-\frac{\mathbf{r}}{\delta^2}\right) \Delta\delta\end{aligned}$$

The total uncertainty of the yaw rate gain is outlined in Table 4.2.

Table 4.2: Total calculated uncertainty using linear approximations.

Parameter	Unit	Nominal Value	Bias Value
δ	deg	4.607	0.5
$\mathbf{r}$	deg/s	10.01	0.01
$G_{\mathbf{r}}$	1/s	2.17	-0.23

5 Results and Discussion

This chapter details the results obtained from the analytical modelling and experimental handling tests.

5.1 Steady State Cornering Response

The understeer gradient, K, was experimentally measured, and expressed in the form of a cornering diagram. Figures 5.1 and 5.2 show the handling diagrams of the vehicle using the constant speed method for lateral acceleration and yaw rate. For this method, the Ackerman steer angle is the neutral steer line. See section 2.1 for a more detail description of the understeer gradient. The experiment was performed at an average longitudinal velocity of 5 m/s (18 kph). The uncertainty error bars have been ommitted as they are smaller than the data points.

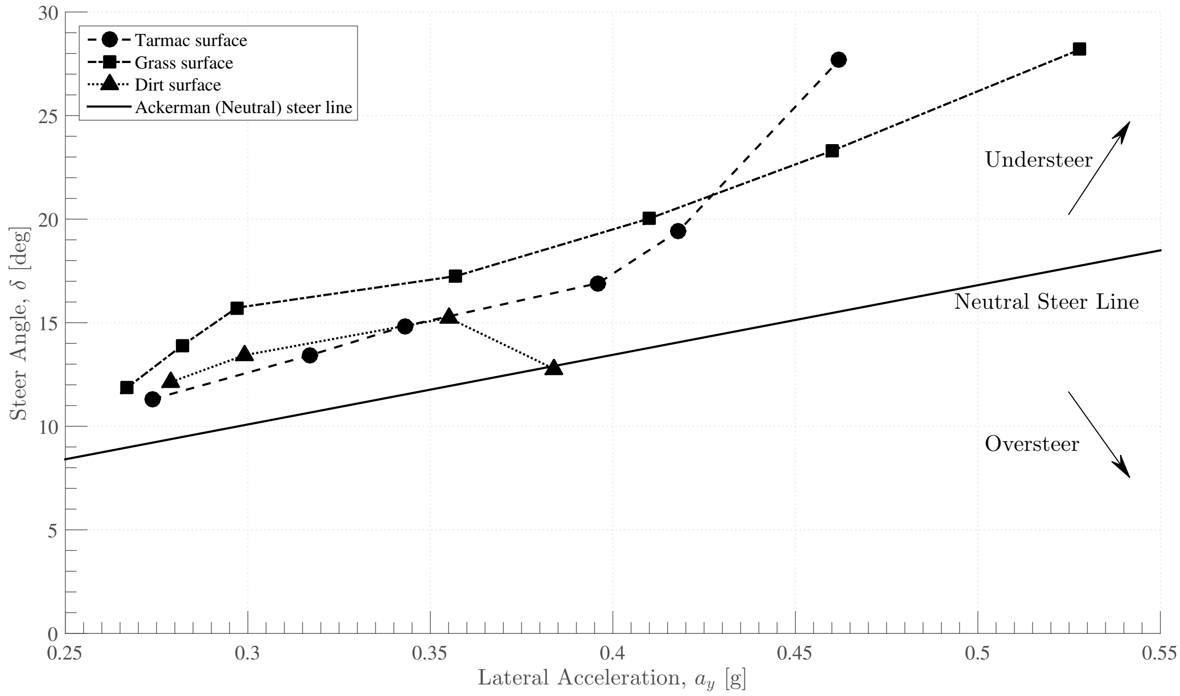

Figure 5.1: Lateral acceleration understeer gradient response.

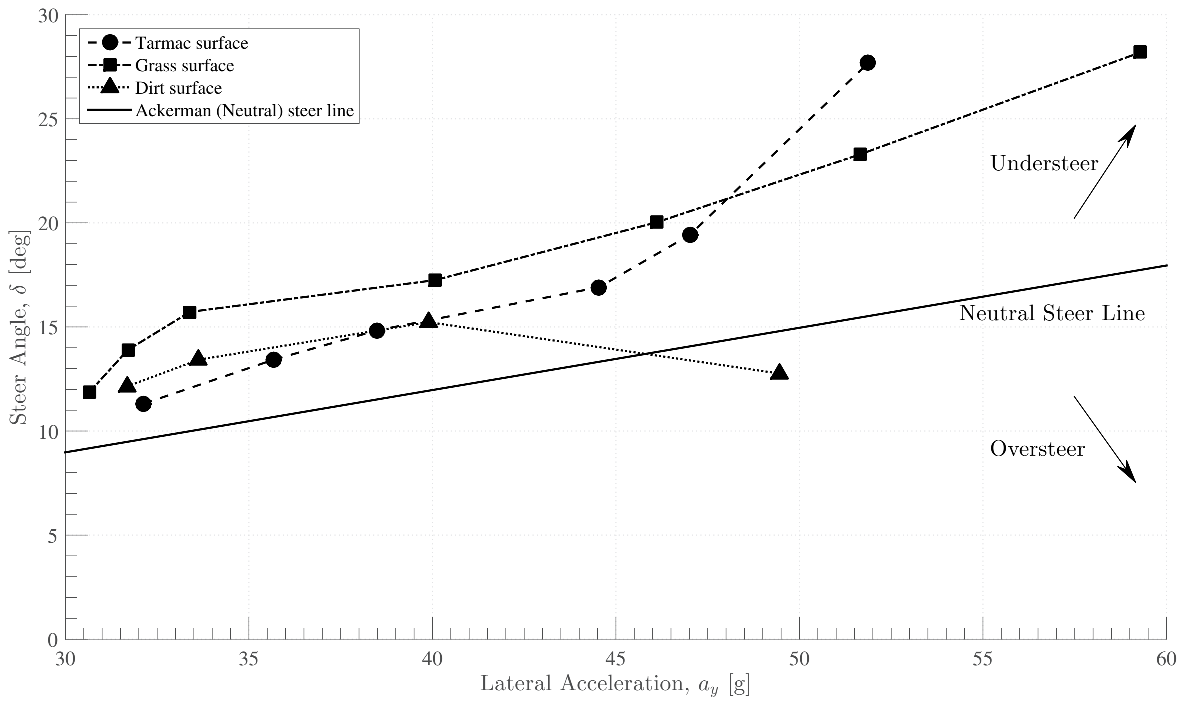

Figure 5.2: Yaw rate understeer gradient response.

The steady state cornering tests were a closed-loop handling test. The differences in surface traction and the influence of the driver on the repeatability error, resulted in differences in understeer gradient at lower lateral accelerations. For lateral accelerations and yaw rates less than 0.35 g and 40 deg/s respectively, the vehicle behaved in a similar manner over each surface type – even though the available traction varies significantly over different surfaces. This is due to the linear tire stiffness at low sideslip angles. When a vehicle performs low lateral acceleration cornering, the lateral forces generated by the tires are insufficient to saturate the tires. At low sideslip angles, the vehicle handling was repeatable, regardless of the surface type. Under high lateral acceleration cornering, the effect of tire stiffness becomes more dominant, and tire saturation will influence the vehicle handling.

When cornering over the tarmac surface, the road surface does not deform due to tire loading. Over the tarmac surface, the vehicle understeers linearly up to 0.38 g and 44.8 deg/s. At a lateral acceleration and yaw rate greater than 0.38 g and 44.8 deg/s, the understeer gradient increases, indicating that the tires cannot linearly generate a lateral force to maintain the turn radius. A larger steering input to maintain the turn radius was required. The vehicle understeers up to a maximum measured lateral acceleration and yaw rate of 0.46 g and 52.1 deg/s respectively.

On the grass surface, the vehicle exhibits stable understeer behaviour up to a lateral acceleration and yaw rate of 0.53 g and 59.5 deg/s respectively. Compared to the tarmac surface, the vehicle was able to maintain a 13% increase in lateral acceleration and 11% increase in yaw rate at a maximum measured steer angle of 28 deg. This was not the expected result. The local cornering stiffness at increased slip angles decreased when on a grass surface, and the limit at which tire saturation occurred was at a larger sideslip angle as compared to the tarmac surface. Below a lateral acceleration of 0.42 g, the understeer gradient on the grass surface was measured to be larger than on the tarmac surface. To achieve the same lateral acceleration, a larger steering input was required. This is again explained by the interpretation that at low sideslip angles, the cornering stiffness of the tires decreased on the grassy surface compared to on the tarmac surface.

The vehicle produced a different handling response on the dirt track surface as compared to on the tarmac or grass surface. Over this surface, an oversteer behaviour was measured, as opposed to the understeer behaviour of the previous surfaces. The vehicle transitioned from understeer to oversteer at a lateral acceleration and yaw rate of 0.35 g and 40 deg/s respectively. The vehicle reached a critical oversteer point at a measured lateral acceleration and yaw rate of 0.39 g and 49.5 deg/s respectively. This is a maximum lateral acceleration and yaw rate decrease of 35% and 4% respectively, compared to on the tarmac surface. The vehicle behaviour beyond this point was unstable, as the vehicle could not maintain the turn radius. On the dirt track surface, the tires reach saturation at a much lower lateral acceleration as compared to on the tarmac or grass surface.

The results indicate that the amount of tire grip is an important aspect in determining vehicle handling quality. On the tarmac surface, the vehicle exhibited the most understeer, and as a result did not posses enough steering to generate a lateral acceleration larger than 0.46 g. On the grass surface, the vehicle exhibited a larger understeer compared to on the tarmac surface, and was able to generate a maximum lateral acceleration of 0.53 g. Below a lateral acceleration of 0.35 g, the vehicle exhibited similar understeer over the dirt track surface compared to the tarmac surface, but at a lateral acceleration greater than 0.36 g, transitioned from understeer to oversteer. On the dirt track surface the vehicle exhibited a maximum measured oversteer at a lateral acceleration of 0.39 g. From a handling perspective, despite requiring larger steering input, handling behaviour on the grass surface is more desirable as the vehicle is able to achieve larger lateral accelerations.

5.2 Step Steering Response

The response to step steering input is useful to evaluate the lateral dynamic behaviour of a vehicle. The yaw rate gain is useful to characterise the vehicle cornering stability. Figure 5.3 shows the steady state yaw rate gain for varying steer input. The open-loop nature of the step steering test resulted in a repeatability error of less than 5% on all three surfaces tested. The error bars due to uncertainty are omitted as they are smaller than the symbols used to plot the data.

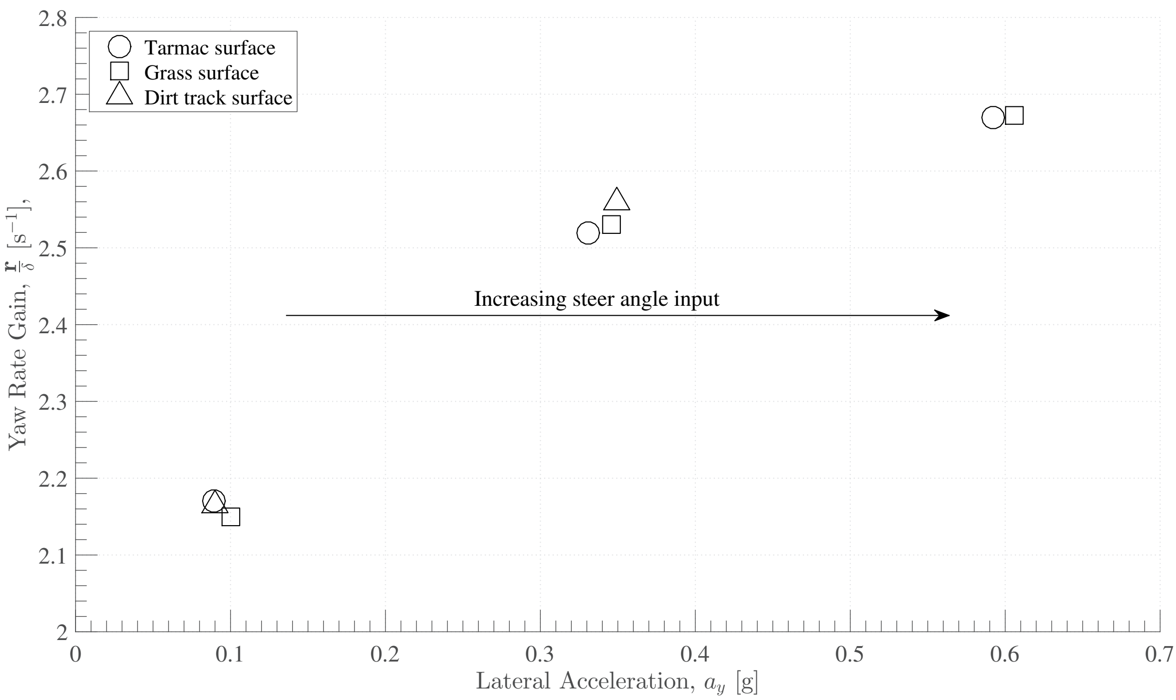

Figure 5.3: Yaw rate gain for increasing steering input.

At a measured lateral acceleration of 0.1 g, the difference in yaw rate gain on the grass and dirt track surfaces were 1.82% and 1.71% as compared to on the tarmac surface. This was expected since the tire grip level had a small influence on vehicle handling at low lateral accelerations. When experiencing low lateral acceleration cornering, the tires need not develop large lateral forces to maintain the turn.

The vehicle achieved a maximum yaw rate gain of 2.52 s^{-1}, 2.53 s^{-1} and 2.56 s^{-1} at a measured lateral acceleration of 0.35 g on the tarmac, grass and dirt track surfaces respectively. Up to a measured lateral acceleration less than 0.35 g, the yaw rate gain was independent of the surface used for testing. The tire cornering stiffness decreased with increasing lateral acceleration, but did not have a large enough influence on cornering performance over the surfaces which offered low tire grip. This supports the results from the steady state cornering tests, which showed similar results on all three surfaces at a lateral acceleration of 0.35 g. The yaw rate gain increased by an average of 17% for all surfaces tested at a lateral acceleration of 0.35 g. Despite the increase in steering input, the vehicle was still operating in a region where handling is stable. The tires are developing sufficient lateral forces to maintain the turn.

The vehicle achieved a maximum yaw rate gain of 2.67 s^{-1} and 2.68 s^{-1} at a measured lateral acceleration of 0.6 g on the tarmac and grass surfaces respectively. The vehicle would not perform the step steer input test at a lateral acceleration of 0.6 g on the dirt track surface due to the oversteer of the vehicle. On the tarmac and grass surface, the vehicle response showed closer similarity than that produced by the steady state cornering tests; a relative difference of 3.2% for a measured lateral accelerations of 0.6 g. The driver had a smaller influence on the repeatability of the open-loop testing procedure than compared to the results of the steady state cornering tests. The yaw rate gain increased by an average of 6% when compared to yaw rate gains measured at a lateral acceleration of 0.35 g. The proportionate decrease in yaw rate gain indicated that the tire grip level had a significant influence on the handling performance. When cornering at higher lateral accelerations, the tires cannot develop sufficient lateral force to maintain neutral steer, and the vehicle understeers at a lateral acceleration of 0.6 g on the tarmac and grass surfaces. This agrees with the similar understeer behaviour determined by the steady state cornering tests at higher lateral accelerations.

The IMU had insufficient bandwidth to measure the transient time delay between the steering input and the lateral acceleration and yaw rate outputs. The response time and yaw overshoot of the vehicle could not be measured. The lower bandwidth, however, did not influence the results of the transient cornering response tests, as the frequency response of the vehicle during the DLC test was within the measurable bandwidth range.

5.3 Transient Cornering Response

The DLC experiment evaluates transient steering input on vehicle handling. The experiment is inherently not as repeatable when compared to handling tests such as the J-turn, or step steering test; the test is a closed-loop manoeuvre which is influenced by the driver. It can therefore be difficult to quantify the differences the road surfaces have on vehicle handling. The DLC experiment is however, representative of an actual driving (and racing) situation, and is very demanding on the vehicle handling response. Figures 5.4 to 5.6 below show the transient response of the vehicle to the DLC over tarmac, grass and dirt conditions respectively.

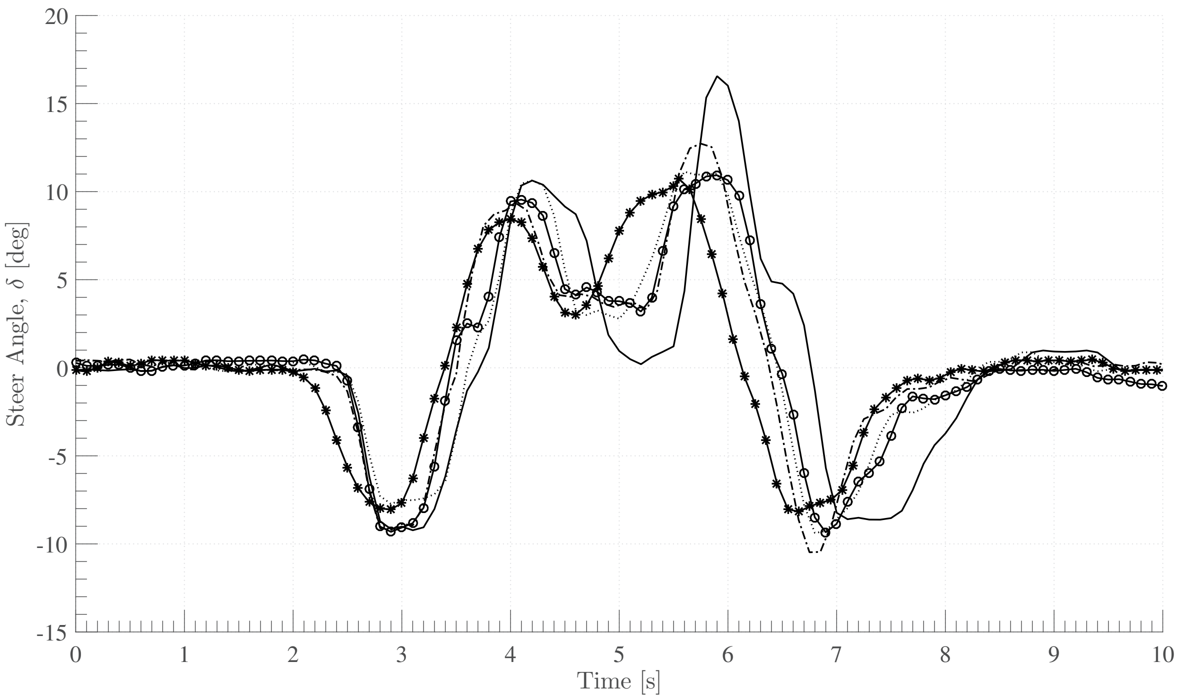

Figure 5.4: Transient response of steer angle to DLC manoeuvre over a tarmac surface.

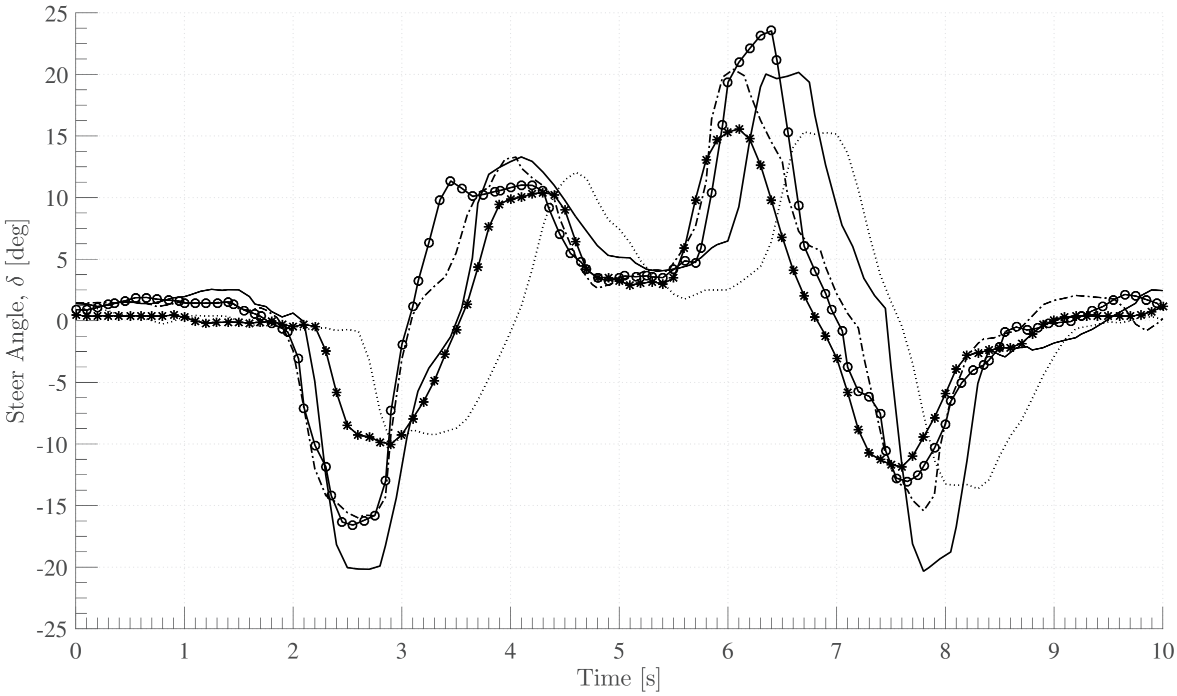

Figure 5.5: Transient response of steer angle to DLC manoeuvre over a grass surface.

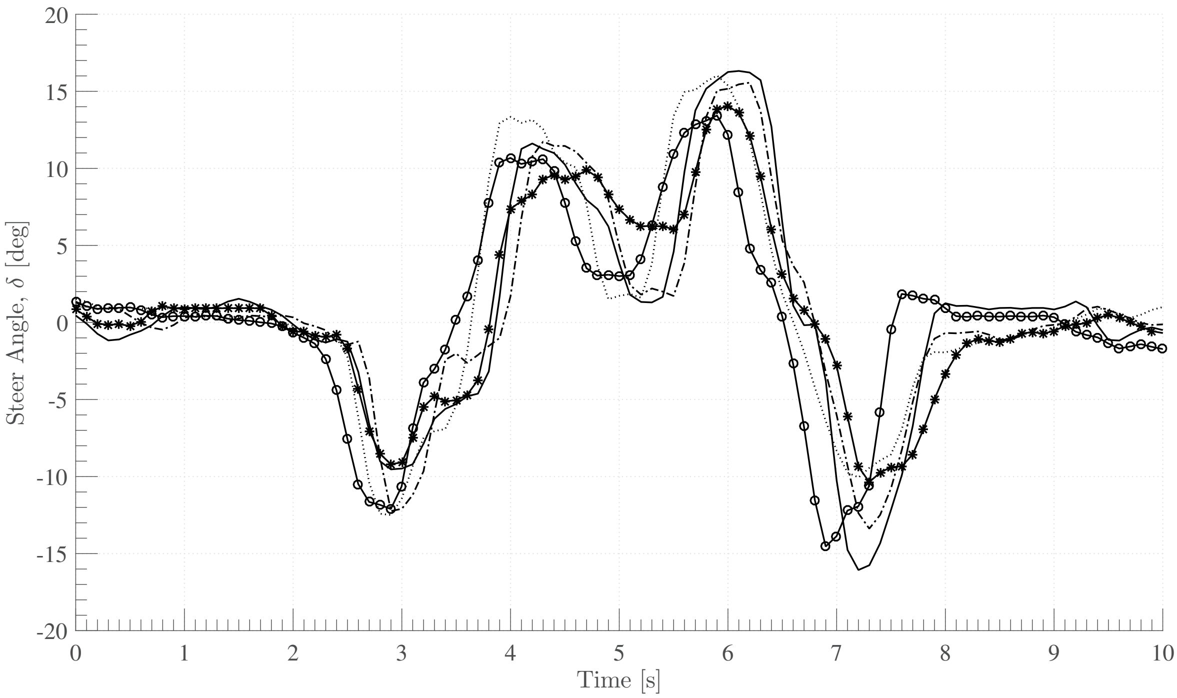

Figure 5.6: Transient response of steer angle to DLC manoeuvre over a dirt track surface.

The influence of the driver skewed the results, making it difficult to distinguish any differences in vehicle response on the different road surfaces. It was also possible that the driver had learned to anticipate the cornering behaviour of the vehicle over time. Thus the turning points of the curves were examined to closer evaluate the differences in vehicle handling caused by differences in road terrain. By looking at the statistical variations in steer angle, lateral acceleration and yaw rate at the turning points, meaningful differences in the vehicle handling were determined. The critical points in the DLC manoeuvre which were analysed were:

1. The initial steer input when moving into the "passing lane", known as "turn in",
2. The steer correction required to correct the course once in the "passing lane", known as "1st correction",
3. The second steer input to move back into the "original lane", known as "turn out", and
4. The second steer correction required to correct the course once in the "original lane", known as "2nd correction".

Figures 5.7, 5.8 and 5.9 respectively show the steer angle, lateral acceleration and yaw rate measured at the critical points. The error bars show the standard deviation of the results obtained from a total of nine experiments which were conducted.

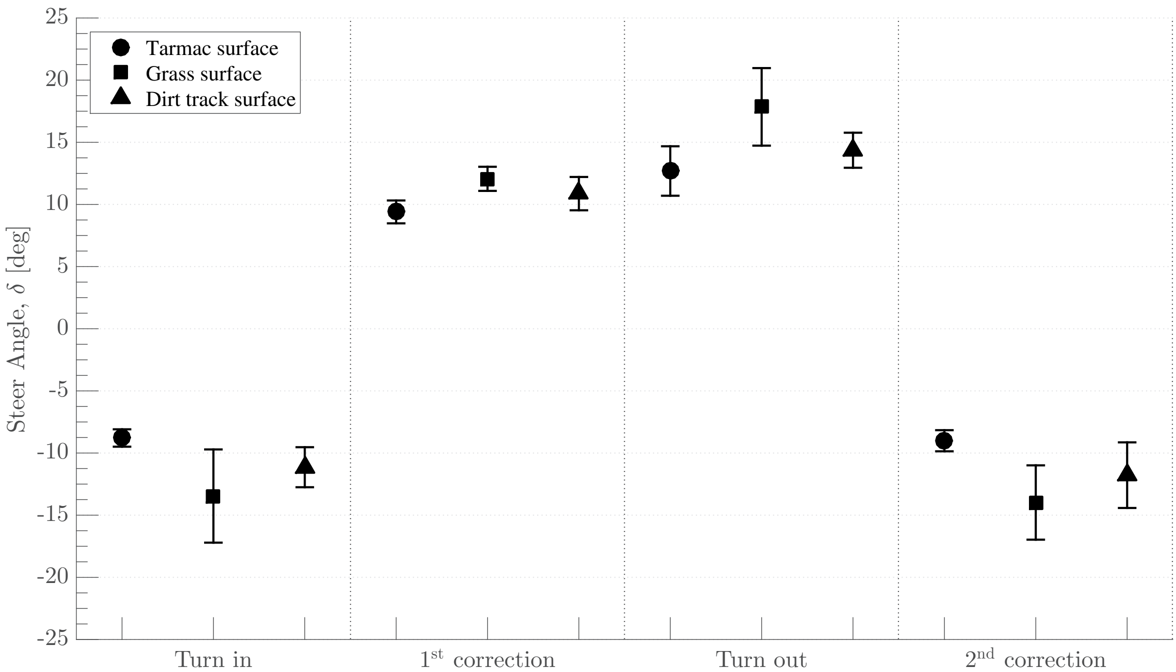

Figure 5.7: Effect of road terrain on steer angle for a DLC experiment.

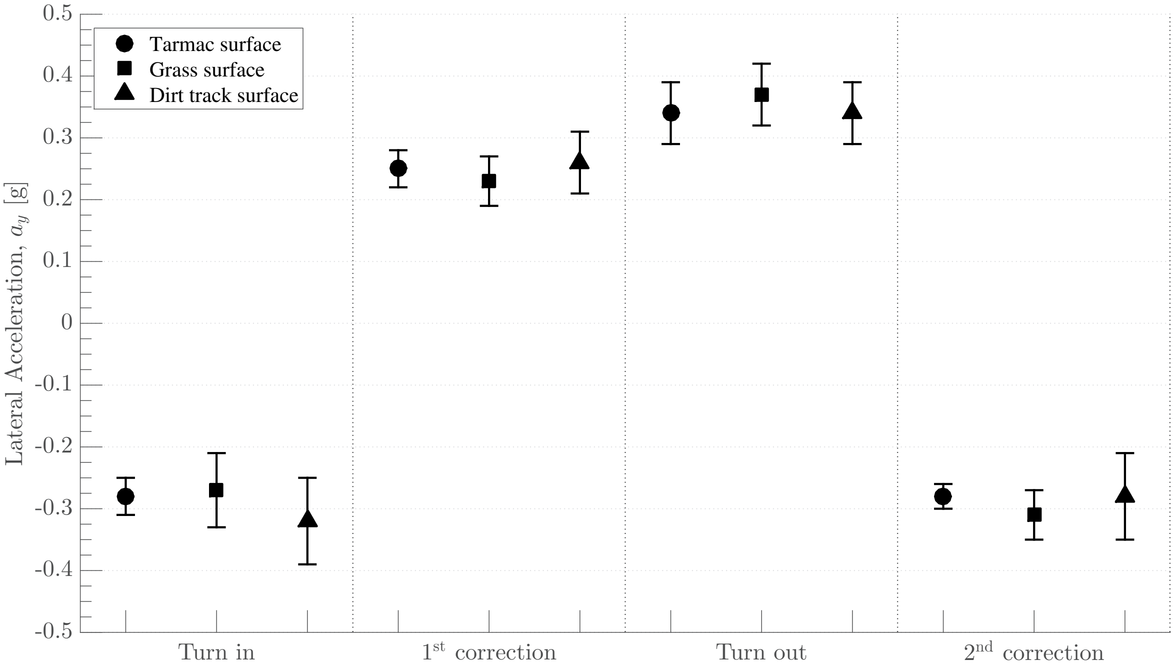

Figure 5.8: Effect of road terrain on lateral acceleration for a DLC experiment.

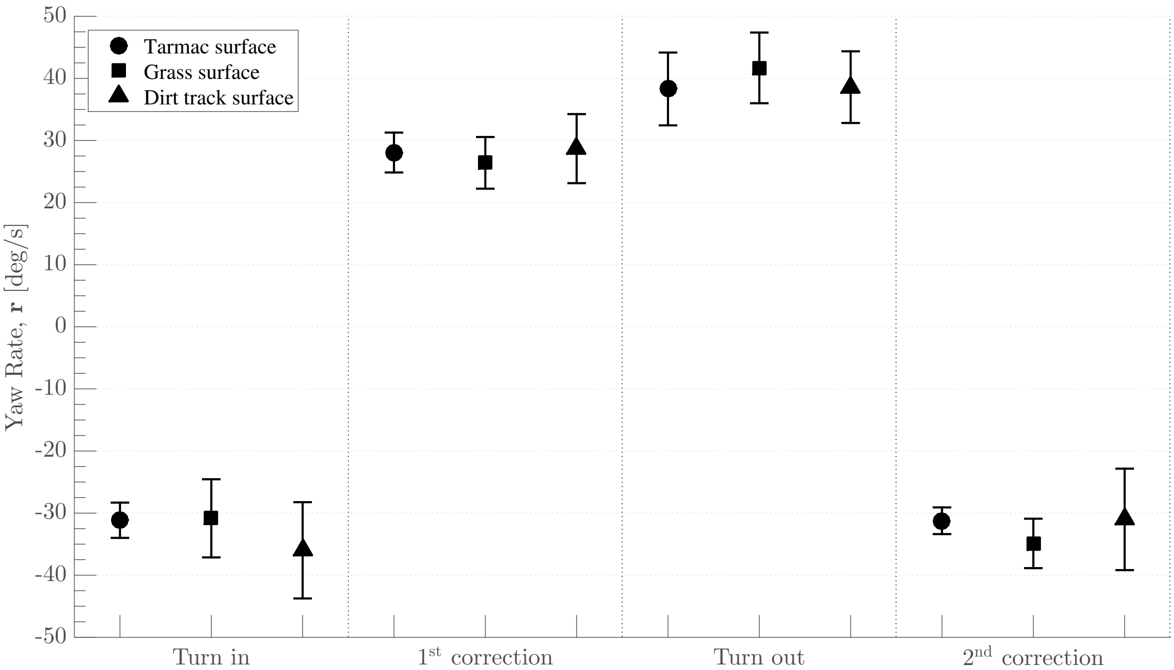

Figure 5.9: Effect of road terrain on yaw rate for a DLC experiment.

Figure 5.7 shows that the vehicle exhibits the most predictability on the tarmac surface. The steering corrections required were much smaller than on the other surfaces, and the deviation was the smallest overall. The measurements from the experiment were repeatable, with low deviation, due to the predictability of the tarmac surface. On the grass surface, the vehicle required an overall larger steering input. The steering deviation on the grass surface was larger than on the tarmac surface. The vehicle behaved somewhat unexpectedly on the grass surface for certain tests and required driver intervention. On the dirt track surface, the experiment produced results of variability lower than on the grass surface. The lateral acceleration and yaw rates must be examined to determine the difference in the vehicle handling.

The steering input required to complete the DLC on the grass surface was between 28% and 55% larger than on the tarmac surface. The lateral acceleration on the grass surface however, only varied by between -5% and 11% compared to on the tarmac surface. As the experiments over a dirt surfaces were performed last, the driver had become used to the handling of the vehicle. After nine tests were performed (not including the practice runs), the driver affected the results by learning to anticipate the handling. On the dirt track surface, the steering input required increased by between 13% and 31% compared to on the tarmac surface, while the lateral acceleration varied only between -1% and 15%. Due to the loss in traction of the tires on grass and dirt surfaces, larger steering inputs were measured than on the tarmac surface.

Figures 5.8 and 5.9 show that the largest lateral accelerations and yaw rates occurred when moving from the passing lane to the original lane; turn out. The average lateral accelerations measured were 0.34 g, 0.36 g and 0.38 g on the tarmac, grass and dirt track surfaces respectively. The average yaw rates measured were 38.0 deg/s, 41.5 deg/s and 39.2 deg/s on the tarmac, grass and dirt track surfaces respectively. Referring back to the steady state cornering diagrams, Figures 5.1 and 5.2 show that during the DLC manoeuvre, the vehicle was operating in the linear understeer region, and handling was predictable. This explains why there was no major differences in handling dynamics. This proves that the vehicle behaves predictably up to the stable limit of approximately 0.35 g, on the surfaces tested.

From the experiments it can be shown that the tires exhibit a linear cornering stiffness up to approximately 0.35 g for all the surfaces tested. On the grass and dirt track surfaces, the tires saturate, producing understeer on the grass surface and oversteer on the dirt track surface.

6 Conclusions

The following conclusions were drawn from the steady state cornering tests, shown in Figures 5.1 and 5.2 respectively:

1. There exists two distinct cornering behaviours; (1) linear understeer up to a 0.35 g lateral acceleration limit, and (2) transition to either understeer on the high tire grip surfaces or uncontrollable oversteer on the low tire grip surface.
2. On the tarmac surface, the vehicle experienced understeer and reached a maximum measured lateral acceleration and yaw rate of 0.46 g and 52.1 deg/s respectively.
3. On the grass surface, the vehicle experienced understeer up to a maximum measured lateral acceleration and yaw rate of 0.53 g and 59.5 deg/s respectively. The 15% increase in lateral acceleration and 14% increase in yaw rate is more desirable for racing, as the vehicle can corner faster on the grass surface compared to on the tarmac surface.
4. On the dirt track surface, the vehicle experienced oversteer at a maximum lateral acceleration and yaw rate of 0.39 g and 49.5 deg/s respectively. There was a decrease in maximum measured lateral acceleration and yaw rate of 36% and 4% respectively as compared to on the tarmac surface. The poor traction offered by the dirt track surface resulted in tyre saturation at a lower lateral acceleration than on the tarmac and grass surfaces.

The following conclusions were drawn from the step steering input test, shown in Figure 5.3 above:

1. The open-loop nature of the step steering test resulted in a repeatability error of less than 5% on all three surfaces tested. The driver had a smaller influence on the repeatability of the open-loop testing.
2. At low lateral accelerations, the tyre grip level had very little influence on handling performance. At a lateral acceleration of 0.1 g, the yaw rate gain on the grass and dirt track surfaces differed by less than 1% as compared to the tarmac surface.

3. Up to a lateral acceleration of 0.35 g, the yaw rate gain was independent of the surface used for testing. At lower lateral accelerations, the tyre grip level did not have a large enough influence on the cornering performance. The tyres are developing sufficient lateral force to maintain the turn.

4. The vehicle would not perform the step steer input test at a lateral acceleration of 0.6 g on the dirt track surface due to the oversteer of the vehicle.

5. At a lateral acceleration cornering of 0.6 g, the tyres were unable to generate sufficient lateral force to maintain neutral steer. On the tarmac and grass surfaces, the disproportionate increase in yaw rate gain showed understeer.

6. The IMU had insufficient bandwidth to capture small transients during testing. The response time and yaw overshoot of the vehicle could not be measured by the IMU.

The following conclusions can be made about the transient performance from the DLC tests, shown in Figures 5.7 through 5.9:

1. This test was a closed-loop manoeuvre due to the significant influence of the driver on the results.

2. The variability of the steering input was the lowest on the tarmac surface, due to the repeatable traction offered. When testing on the grass and dirt track surface, the available traction decreased, and the variability of the steering input increased. Greater steering effort had to be applied by the driver on the grass and dirt track surface.

3. The largest lateral accelerations and yaw rates were experienced when moving from the passing lane to the original lane; turn in. The maximum measured lateral accelerations were 0.34 g, 0.36 g and 0.38 g on the tarmac, grass and dirt track surfaces respectively. The average yaw rates were 38.0 deg/s, 41.5 deg/s and 39.2 deg/s on the tarmac, grass and dirt track surfaces respectively.

4. The vehicle was operating in a region of relatively stable handling performance. In this region, the tyres were not saturated and were still able to provide predictable performance.

5. Due to the loss in traction of the terrain, the steering input required increased by between 28% and 55% on the grass surface when compared to the tarmac surface, and between 13% and 31% on the dirt track surface when compared to the tarmac surface.

6. The IMU bandwidth did not influence the DLC results, as the frequency response of the vehicle was within the measurable bandwidth range.

7. The use of closed-loop experiments to determine handling characteristics resulted in skewed data due to driver influence on the vehicle response. Open-loop experiments yielded results of lower variance.

The handling performance on the tarmac surface was repeatable for all the cornering tests performed. On the grass surface, the cornering stiffness of the tyres decreased, resulting in an increase in steering variability when exposed to transient cornering. On the grass and dirt track surface, the tyres were able to generate sufficient lateral force to obtain understeer up to a maximum lateral acceleration of 0.6 g. Up to a maximum lateral acceleration of 0.35 g, the tyre grip level was still sufficient that the handling was stable on the grass and dirt track surfaces as compared to on the tarmac surface. On the dirt track surface, the tyre traction decreased at a lateral acceleration of 0.35 g and the vehicle exhibited oversteer at a maximum lateral acceleration of 0.39 g. The tyres were unable to develop sufficient lateral force on the dirt track surface for high lateral acceleration manoeuvres. When performing transient cornering, the ability of the tyres to develop a lateral force had the biggest influence on handling on surfaces which offered low tyre traction.

7 Recommendations

The recommendations for future work are as follows:

1. Investigate the effect of varying tire parameters on the cornering stiffness over tarmac surfaces. Adapt the current setup to also include the measurement of tire pressure and temperature between experiments. tire pressure was not accounted for but can result in large differences in handling behaviour. The tire pressure was maintained constant for all tests to reduce variation.
2. Develop a tire model for the BMG Wits Baja vehicle for tarmac surfaces. This can then be used in the investigation of vehicle dynamics modelling. The comparison of experimental data with analytical models should be investigated.
3. Upgrade the DAQ to utilise a more powerful micro-processor. Maintaining the small form-factor and portability of the system whilst increasing sampling rate could be possible without significant changes to the experimental setup.
4. The use of a global positioning system (GPS) would provide a more accurate measurement of vehicle speed.

References

[1] SAE. *Baja SAE*. http://students.sae.org/cds/bajasae/. Accessed 17 January 2015. 2015.

[2] University of the Witwatersrand. *BMG Wits Mini Baja*. https://www.facebook.com/witsbaja. Accessed 20 January 2015. 2014.

[3] L. D. Metz. 'What Constitutes Good Handling?' In: *SAE Motorsports Engineering Conference and Exhibition* 724 (2004), p. 10. DOI: 10.4271/2004-01-3532.

[4] J. C. Brown et al. 'Recreational Off-highway Vehicle (ROV) Handling and Control'. In: *SAE Paper 2012-01-0239* (2012).

[5] D. Renfroe et al. 'Reconciliation of ATV/UTV Handling Characteristics and the Operator'. In: *SAE Paper 2014-01-0095* (2014).

[6] F. J. P. Pujatti et al. 'Longitudinal Performance of a BAJA SAE Vehicle'. In: *SAE Paper 2010-36-0315* 7 (2010).

[7] S. Kakria and M. Wagh. 'Modeling and Simulation Study of BAJA SAE India All Terrain Vehicle (ATV) Using Integrated MBD-FEA Approach'. In: *SAE Paper 2015-26-0219* (2015).

[8] C. B. Amaral and C. R. S. Neto. 'Validation of a Mathematical Model that Studies the Critical Steering Angle for a Lateral Rollover on a Baja SAE Vehicle'. In: *SAE Paper 2011-36-0186* (2011).

[9] P. S. Els and P. H. Cronjé. 'Improving Off-road Vehicle Handling using an Active Anti-roll Bar'. In: *Journal of Terramechanics* 47 (2010), pp. 179–189.

[10] J. A. Pytka et al. 'An Instrumented Vehicle for Off-road Dynamics Testing'. In: *Journal of Terramechanics* 48 (2011), pp. 384–395.

[11] D. I. Katzourakis et al. 'Race-car Instrumentation for Driving Behavior Studies'. In: *IEEE Transactions on Instrumentation and Measurement* 61.2 (2012), pp. 462–474. ISSN: 00189456. DOI: 10.1109/TIM.2011.2164281.

[12] J. B. Stewart and E. H. Law. 'Investigation of Rollover, Lateral Handling, and Obstacle Avoidance Manoeuvres of Tactical Vehicles'. In: *SAE Paper 2006-01-3569* (2006), p. 13. DOI: 10.4271/2006-01-3569.

[13] P. S. Els, P. E. Uys and M. Thoresson. 'Suspension Settings for Optimal Ride Comfort of Off-road Vehicles Travelling on Roads with Different Roughness and Speeds'. In: *Journal of Terramechanics* 44 (2007), pp. 163–175.

[14] R. Antônio et al. 'Vibration and Noise Exposure Level in an Off-road Prototype'. In: *SAE Paper 2006-01-2546* (2006).

[15] A. T. Owens, M. D. Jarmulowicz and P. Jones. 'Structural considerations of a Baja SAE Frame'. In: *SAE Paper 2006-01-3626* (2006).

[16] W. F. Milliken and D. L. Milliken. *Race Car Vehicle Dynamics*. Second Edi. Vol. 1. Warrendale, USA: Society of Automotive Engineers, 1995, p. 1000. ISBN: 1560915269.

[17] T. D. Gillespie. *Fundamentals of Vehicle Dynamics*. Warrendale, USA: Society of Automotive Engineers, 1992, p. 519. ISBN: 1560911999. DOI: 10.4271/R-114.

[18] ISO. 'Passenger Cars – Steady-state Circular Driving Behaviour – Open-loop Test Methods'. In: *ISO 4138-1:2012* (2012).

[19] ISO. 'Road vehicles – Lateral transient response test methods – Open-loop test methods'. In: *ISO 7401:2011* (2016).

[20] ISO. 'Passenger Cars – Test Track for a Severe Lane-change Manoeuvre – Part 1: Double Lane Change'. In: *ISO 3888-1:1999* (2009).